Interference Protection Criteria Simulation

Robert J. Achatz

Institute for Telecommunication Sciences, National Telecommunications and Information Administration, Boulder, CO, USA

Abstract— **Interference protection criteria (IPC) determine the interfering signal power a system can tolerate when sharing spectrum with other services. IPC are typically determined by measurements, but good measurements are often hindered by restrictions on equipment availability and inaccessible equipment signals, performance metrics, and operational parameters. The purpose of the research described in this article is to determine if these difficulties can be avoided by replacing IPC measurements with software simulations. Our approach is to use commercial off-the-shelf (COTS) radio system simulator software to model previous IPC measurement test fixtures and compare simulated to measured results. Measurements of mutual interference between radar and LTE systems are compared. The comparison shows that simulation can be a viable alternative to IPC measurement.**

Keywords— Citizens Broadband Radio Service, electromagnetic compatibility analysis, interference protection criteria, LTE, SPN-43C radar, radio system software simulation, spectrum engineering, spectrum sharing

I. INTRODUCTION

In today's spectrum sharing scenarios, interference is allowed as long as the performance of the system experiencing interference ("the victim system") is not significantly degraded. To minimize the probability of interference, spectrum planners separate the systems in distance and frequency. The amount of separation is determined by interference protection criteria (IPC) which specify the allowed interference power at a specific center frequency offset [1].

Engineers at the National Telecommunications and Information Administration (NTIA) Institute for Telecommunication Sciences (ITS) typically estimate IPC with measurements of operational equipment in the laboratory or field with the setup shown in Fig. 1. The basic IPC measurement method is:

1. Set victim received signal power to a baseline signal to noise ratio (SNR) corresponding to typical interference-free performance
2. Set interfering signal power, I, to the lowest interfering signal power of interest
3. Measure performance
4. Incrementally increase I and repeat step 3 to the highest I of interest

This method is repeated at various frequency offsets if needed.

Fig. 2 shows how results of an IPC measurement are typically presented. The allowed interfering signal power, I_a, or interfering-signal to noise power ratio, INR_a, corresponding to

the allowed performance degradation is identified by the spectrum sharing stakeholders after careful review of the measurement results.

These measurements are often hindered by restrictions on equipment availability. In some cases the systems involved have not even been built so measurements are not possible. In other cases the systems can only be tested for a brief period of time to avoid service interruptions. The measurements are also hindered by inaccessible equipment signals, performance metrics, and operational parameters. All of these factors can make accurate and repeatable measurements difficult to obtain by other interested parties. The purpose of this work is to determine if these obstacles can be avoided by replacing laboratory or field measurements with software simulations. Our approach is to use commercial off-the-shelf (COTS) radio system simulator software to model previous IPC measurement test fixtures and compare simulated to measured results. Complete details of this work are provided in [2].

Currently, there is considerable interest in Long Term Evolution (LTE) cellular radio systems sharing spectrum with Federal radars in the 3.5 GHz Citizen Broadband Radio System (CBRS) band [3],[4]. NTIA's Office of Spectrum Management
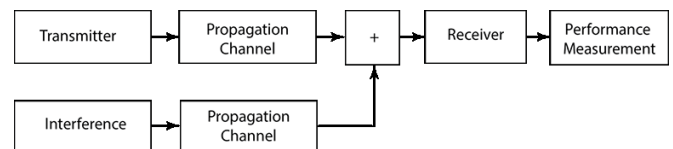

Fig. 1. General IPC measurement setup. Desired and interfering signals go through independent propagation channels since their transmitters are generally not co-located.
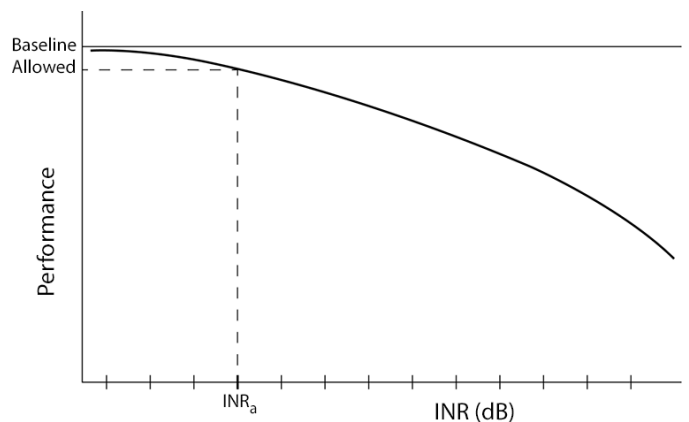

Fig. 2. Graph showing how results of an IPC measurement at a specific frequency offset are typically presented. Baseline performance is evaluated without interference. The IPC is the allowed INR, INR_a.

(OSM) and ITS have conducted a number of IPC measurements for various cases of this sharing scenario [5]-[7]. Here, we will focus on comparing measured results between LTE frequency division duplex (FDD) and SPN-43C shipborne radar equipment.

II. Scenario

The interference scenario, depicted in Fig. 3, shows an LTE/FDD evolved node-B (eNB) transmitting to a LTE/FDD user equipment (UE) over what is referred to as its downlink. At the same time, the SPN-43C radar is transmitting a signal whose received reflection determines the location of the target. This work will focus on interference created by the radar signal when received by the LTE/FDD UE [6] and the LTE/FDD eNB signal when received by the radar [7].

The IPC measurements evaluated in this work impose the following restrictions on the scenario: all propagation paths are free of fading, radar targets are stationary with non-fluctuating, Swerling 0 radar cross sections (RCS), there are no radar clutter returns from precipitation, terrain, buildings, or vegetation, and the LTE/FDD eNB signal is emulated by Gaussian noise (GN).

As shown in Fig. 4, the SPN-43C and LTE/FDD signals have no center frequency offset and the SPN-43C bandwidth is less than the LTE/FDD signal bandwidth. The LTE/FDD signal power is the average power at the receiver input. The SPN-43C signal power is the peak power at the receiver input. The receiver noise and Gaussian interference powers are the average power after receiver detection filtering but referred to the receiver input.

III. Equipment Description

A. LTE Equipment Description

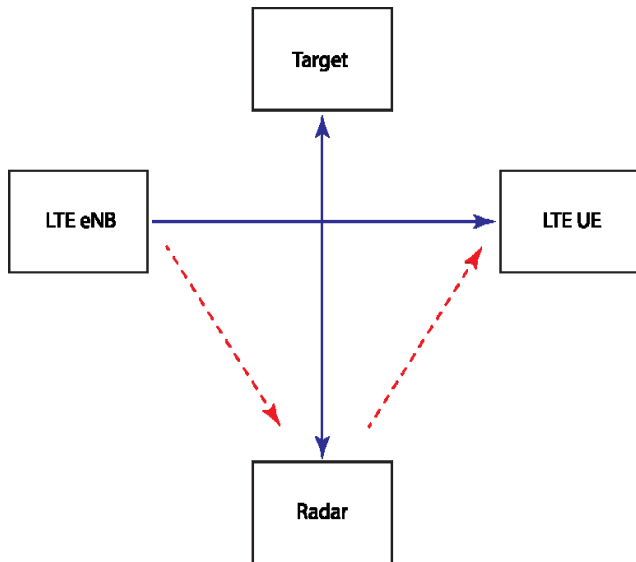The LTE/FDD downlink uses orthogonal frequency division multiple access (OFDMA) to send messages with orthogonal frequency division modulation (OFDM) from the LTE/FDD eNB to a number of UEs. Data and overhead are organized into physical layer 10 ms frames and 1 ms subframes composed of ½ ms, 180 kHz wide resource blocks (RB).

For the downlink the data is carried by physical downlink shared channels (PDSCH). Overhead information is carried over the physical downlink control channel (PDCCH) and the physical broadcast channel (PBCH). Overhead signals include the secondary synchronization signal (SSS), primary synchronization signal (PSS), and the common reference signal (CRS).

The LTE/FDD media access control (MAC) layer presents data and overhead to the physical layer in discrete transport blocks (TB). Every millisecond, a scheduler allocates a sufficient number of RBs to accommodate TB transmission.

The scheduler uses adaptive modulation and coding scheme (AMCS), rank adaptation, and hybrid automatic repeat request (HARQ) functions to maximize spectrum efficiency. AMCS matches various modulation and coding schemes (MCS) composed of 32 combinations of forward error correction (FEC) codes and modulation-orders to radio channel conditions. Spectral efficiency generally increases with MCS index. Rank adaptation determines the most appropriate number of independent data streams referred to as layers or ranks and corresponding multiple antenna technique. HARQ manages TB retransmission.

All these functions require feedback from the UE to the eNB. UE AMCS and rank adaptation functions estimate SNR and channel impulse response for channel quality indicator (CQI) and rank indicator (RI) feedback. HARQ computes the cyclic redundancy check (CRC) for block error feedback.

B. SPN-43C Equipment Description

The SPN-43C radar, designed and first operated in the 1960s, is a remarkably simple radar. The radar transmits a simple repetitive "on-off" carrier pulse train from a rotating 2 degree beamwidth antenna. Pulse width, pulse repetition interval (PRI), and antenna rotation period are nominally 1 μs, 1 ms, and 4 s, respectively. When the pulse is not being

Fig. 3. Interference Scenario. Blue lines indicate desired signals and dashed red lines indicate interfering signals.
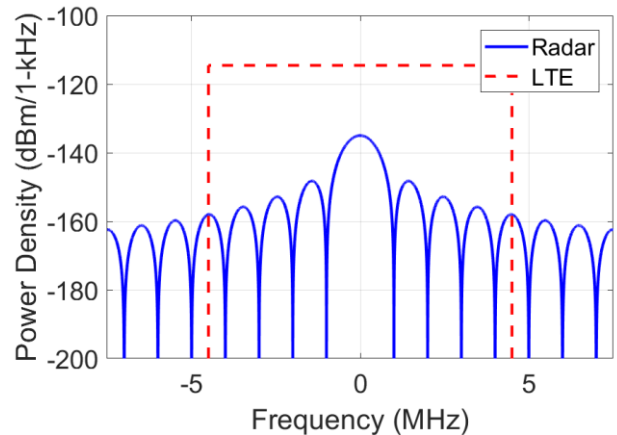
Fig. 4. Ideal SPN-43C radar and LTE/FDD eNB power spectral densities for -75 dBm peak radar and average LTE powers.

transmitted the receiver listens for pulses reflected from aircraft in the sky. The received pulses are detected, non-coherently integrated to enhance SNR, compared to a manually set threshold, and displayed as a 'blip' on a planned position indicator (PPI) display. Approximately 20 pulses can be integrated in the time the rotating antenna beamwidth traverses a point target.

Additional SPN-43C signal processing consists of automatic gain control (AGC), sensitivity time control (STC) short range clutter mitigation, and fast time constant (FTC) precipitation clutter mitigation. While some SPN-43C radars have moving target indication (MTI), clutter rejection, and constant false alarm rate (CFAR) signal processing functions, the radar that was measured did not have them.

IV. IPC MEASUREMENT AND SIMULATION MODEL

A. LTE/FDD UE IPC Measurement and Simulation Model

The LTE/FDD UE IPC measurements were performed in the laboratory. The test fixture had two eNB transmit and two UE receive paths connected by cables and operating in open loop spatial multiplexing transmission mode (TM) 3. Interference was added to each path with independent signal generators.

The measurements were executed over a 10 MHz LTE downlink channel with 50 RB. Each OFDMA subframe had 3 PDCCH. The baseline signal power was set at -75 dBm corresponding to a 22.5 dB SNR to obtain a 50 Mbps throughput.

AMCS was enabled but MCS never exceeded 23. TM-3 rank adaptation allowed up to two independent data streams. While HARQ allowed up to three retransmissions, post-measurement analysis is based on first transmission throughput and block error rate (BLER) averaged over 2000 TBs.

The simulation model emulated all the test fixture features with the following exceptions. First, the measured equipment's AMCS tables relating SNR, CQI, and MCS were not known so simulated values were used.

Second, the simulation model only allowed the SNR for CQI assignment to be estimated from the PSS or set by a previously calculated "ideal" value. We used the SNR estimate from the PSS. We do not know how the measured equipment determined SNR for CQI assignment.

Third, the simulation model did not include rank adaptation. However, fixing the rank at 2 was not a problem since measurement rank rarely deviated from 2.

Fourth, the model used 0 HARQ retransmissions so simulation results would not have to be post-processed for first transmission throughput and BLER.

Fifth, data and overhead powers relative to CRS power were 0 dB with the exception of the PSS and SSS which were 10 dB. Corresponding measured equipment power ratios were not known.

B. SPN-43C IPC Measurement and Model

The SPN-43C IPC measurement was performed in the field at a radar test facility using a visual PPI display performance measurement method. This method was developed primarily because of difficulties encountered in the past using custom built in test equipment (BITE) methods. In some cases operators trained in using the BITE function were not available. In other cases the radars did not have BITE functions.

The visual method generates 10 test targets along the PPI radial every antenna rotation. The test engineer visually counts the number of targets discernable on the PPI display for 20 antenna rotations. The probability of detection (P_d) is the number of targets discerned divided by 200. Probability of false alarm (P_{fa}) is impractical to count visually.

The baseline interference free state was set by first adjusting the threshold and then adjusting the signal power. The threshold was set so that only a small number of false alarms were visible on the PPI display corresponding to an approximate 10^{-5} P_{fa}. The threshold was not allowed to be adjusted during the IPC measurement. SNR was set to correspond to a 0.9 P_d. Signal and noise powers were not independently measured. While AGC was enabled, STC and FTC were disabled.

The simulation model used square law detection, analog moving window non-coherent integration, and provided both P_d and P_{fa}. Assuming a 0 dB noise figure, baseline conditions were obtained with a 12.8×10^{-12} V^2 threshold and a 2.7 dB SNR. One million Monte Carlo P_{fa} trials were executed so that approximately 10 false alarms would occur at baseline. The corresponding number of P_d trials was 1000.

AGC, STC, and FTC functions were not implemented because the interference did not overload the measured receiver and there was no clutter present.

V. IPC RESULTS COMPARISON

A. LTE/FDD UE IPC Results Comparison

Simulated SNR, CQI, and MCS values were first determined. The values were acquired with GN while operating in TM-3 to emulate measurement conditions. Results, shown in Table 1, correspond to that of a single input single output (SISO) channel as expected [8], [9].

Table 1. SNR, CQI, and MCS values derived from simulation.

Minimum SNR (dB)	CQI	MCS
-4.7	1	0
-3.5	2	2
-2.2	3	4
-0.9	4	6
1.0	5	8
2.8	6	10
4.1	7	12
5.9	8	14
7.3	9	16
9.5	10	18
11.2	11	20
12.6	12	22
14.8	13	24
16.8	14	26
18.0	15	27

Next, the AMCS function was tested with GN interference. The results show similar behavior. However there are notable differences. For example, results in Fig. 5 show that simulation can tolerate more interference power than the measurements for the same throughput. This difference becomes most pronounced from -93 to -87 dBm. Since Fig. 6 shows nearly identical MCS at -90 and -87 dBm, the differences seem to be caused by more than UE SNR estimation and CQI assignment.

Finally, the IPC simulation for SPN-43C interference was performed. Since the pulse repetition period was identical to the subframe period it was possible to repeatedly place the pulse on the same OFDM symbol as shown in Fig. 7.

Fig. 8 compares simulated throughput with the pulse placed on the PSS with measured throughput with unknown pulse placement. Simulated throughput clearly degrades much faster than the measured throughput. This disparity is underscored by the drastic differences in MCS in Fig. 9. Simulations with pulses on the other OFDM symbols maintain the highest MCS, since SNR estimation is not affected by the interference, but fail catastrophically by -65 dBm.

B. SPN-43C IPC Results Comparison

Simulated results in Fig. 10 show P_d and P_{fa} increasing with interference. The unexpected P_d result, which has been analytically verified, is in clear contrast to those of radars with CFAR where P_d degradation is attributed to the interference raising the threshold to maintain a constant P_{fa}. The most likely reason the measured P_d results diverge from the simulated results is that the measured targets are subjectively judged absent when obscured by false alarms.

VI. CONCLUSIONS

Although the simulated LTE/FDD UE behaved similarly to the measured UE with GN interference the simulation was not able to reproduce measured behavior with SPN-43C interference.

Interestingly, the measured SPN-43C interference results showed full throughput at -70 dBm interference power corresponding to a -5 dB signal to interference ratio (SIR) and maintained relatively robust performance at even lower SIR. This is in stark contrast to the simulated results which required -85 dBm or a 10 dB SIR for full throughput and degraded to 30% full throughput by -5 dB SIR.

While the simulation results agree with recent field measurements [10], the robust performance shown by the measured equipment could be due to pulsed interference mitigation [11]. Further work is needed to clarify this discrepancy.

The SPN-43C simulations showed that radars with manually set thresholds should be evaluated with a P_{fa} performance metric. Since it is impractical to measure P_{fa} visually, simulation is clearly the best choice for determining IPC of radars with manually set thresholds.

IPC simulation undoubtedly removed problems with equipment availability and inaccessible equipment signals, performance metrics, and operational parameters. While problems were encountered replicating SPN-43C interference
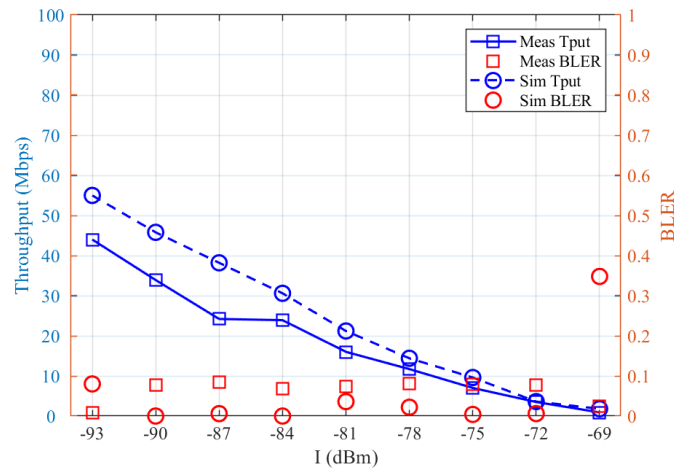

Fig.5.   LTE/FDD UE throughput and BLER with GN interference.
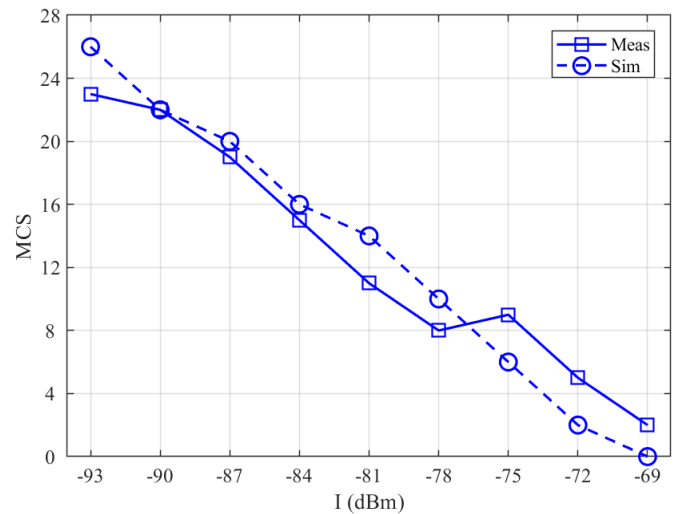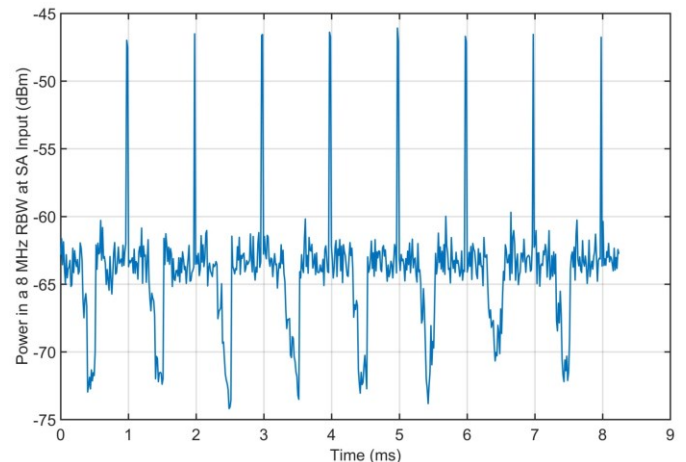

Figure 6. LTE/FDD UE MCS with GN interference.

Figure 7. Pulsed interference on LTE signal from measurements.
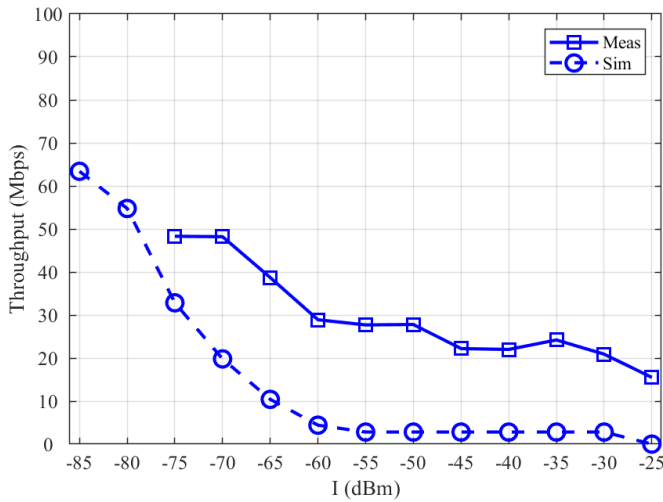
Figure 8. LTE/FDD UE throughput with SPN-43C radar interference.
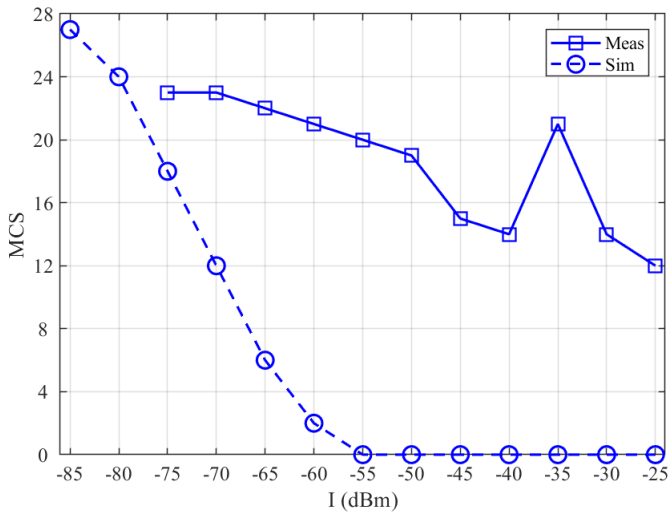

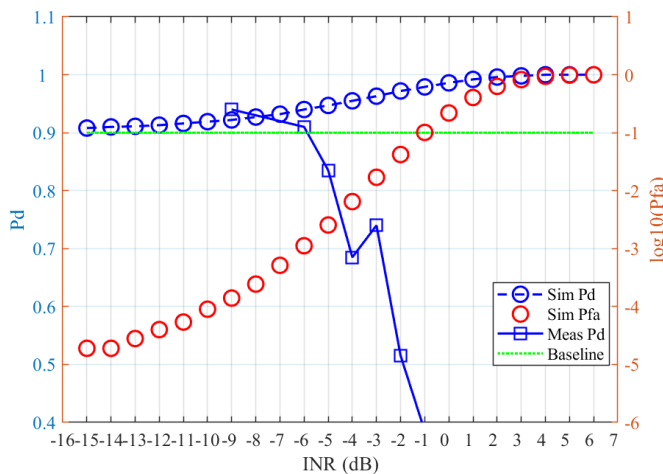Figure 9. LTE/FDD UE MCS with SPN-43C radar interference.

Fig.10. Results for SPN-43C radar with LTE/FDD eNB interference emulated by GN.

in the LTE/FDD UE they can likely be eliminated with more study. Simulation offered much better accuracy for LTE/FDD eNB interference into the SPN-43C radar. Thus our work shows that, with some effort, simulation can be a viable alternative to IPC measurement.

ACKNOWLEDGMENT

Brent Bedford, formerly with the Institute for Telecommunication Sciences, provided invaluable assistance throughout the course of this work.

REFERENCES

[1] Paul et. al., "Interference protection criteria," U.S. Dept. of Commerce, NTIA Report 05-432, October 2005, http://www.its.bldrdoc.gov/publications/2462.aspx.

[2] R. J. Achatz and B. Bedford, "Interference protection criteria simulation," U.S. Dept. of Commerce, NTIA Report, forthcoming.

[3] FCC Further Notice of Proposed Rule Making, Proposes Creation of New Citizens Broadband Radio Service in 3.5 GHz, Federal Communications Commission, Washington D.C., USSA, FCC 14-49, GN docket no. 12-354, Apr. 2014.

[4] U.S. Dept. of Commerce, NTIA, "An Assessment of the Near-Term Viability of Accommodating Wireless Broadband Systems in the 1675-1710 MHz, 1755-1780 MHz, 3500-3650 MHz, and 4200-4220 MHz, 4380-4400 MHz Bands," Oct. 2010, https://www.ntia.doc.gov/report/2010/assessment-near-term-viability-accommodating-wireless-broadband-systems-1675-1710-mhz-17.

[5] F. Sanders, J. Carroll, G. Sanders, and R. Sole, "Effects of Radar Interference on LTE Base Station Receiver Performance," U.S. Dept. of Commerce, NTIA Report 14-499, Dec. 2013, https://www.its.bldrdoc.gov/publications/2742.aspx.

[6] G. Sanders, J. Carroll, F. Sanders, R. Sole, "Effects of Radar Interference on LTE (FDD) eNodeB and UE Receiver Performance in the 3.5 GHz Band," U.S. Dept. of Commerce, NTIA Report 14-506, July 2014, https://www.its.bldrdoc.gov/publications/2759.aspx.

[7] F. Sanders, J. Carroll, G. Sanders, R. Sole, R. Achatz, L. Cohen, "EMC measurements for spectrum sharing between LTE signals and radar receivers," U.S. Dept. of Commerce, NTIA Report 14-507, July 2014, https://www.its.bldrdoc.gov/publications/2760.aspx.

[8] M.T. Kawser, N.I. Bin-Hamid, M.N. Hasan, M.S. Alam, and M. M. Rahman, "Downlink SNR to CQI Mapping for Different Multiple Antenna Techniques in LTE," International Journal of Information and Electronics Engineering, Vol. 2, No. 5, Sept. 2012, pp. 757-760.

[9] C. Mehlfuhrer, M. Wrulich, J.C. Ikuno, D. Bosanska, and M. Rupp, "Simulating the Long Term Evolution Physical Layer," in Proc. of the 17th European Signal Processing Conference, Glasgow, Scotland, Aug 24-28, 2009, pp. 1471-1478.

[10] J.H. Reed, A.W. Clegg, A.V. Padaki, T. Yang, R. Nealy, C. Dietrich, C.R. Anderson, and D.M. Mearns, "On the Co-Existence of TD-LTE and Radar Over 3.5 GHz Band: An Experimental Study," IEEE Wireless Communications Letters, Vol. 5, No. 4, Aug. 2016, pp. 368-371.

[11] H. Safavi, C. Ghosh, E. Visotsky, R. Ratasuk, and S. Roy, "Impact and Mitigation of Narrow-band Radar Interference in Down-link LTE," in Proc. of the IEEE ICC 2015 Wireless Communications Symposium, pp. 2644-2649.